Slope's similarity of the Eastern and the Western steeps of the two Lebanese mountain ranges

Naji Kehdy*

Abstract.

Technical development represented by DEM allows the application of statistical models, to answer a large number of different scientific problems. Among these statistical models, we distinguish the spatial PCA model, which was applied in this study, to the eastern and western slopes of the two mountain ranges of Lebanon. The application of this model on some of the slope's characteristics helped to classify them by degree of similarity. The results showed, contrary to the southern regions, that the northern regions are similar to each other. These results helped to point out Dubertret's supposition, in which he assumes that these slopes are dissimilar.

Keywords: Spatial PCA, Dubertret's theory, Mount-Lebanon, Anti-Lebanon.

Introduction

Defined as a mathematical method, the principal component analysis (PCA) is used to reduce the dimension of a data set consisting of a large number of interrelated variables (Prasad Mishra, Swain, Laishram, & Taraphder, 2017). This method, which is considered one of the oldest techniques (Hotelling, 1933; Pearson, 1901), gained its importance when it is used from a geographical and geological approach (Berry, 1964; Hägerstrand, 1969; Tinkler, 1972; Johnston, 1978; Davis, 1986), where spatial data which consist of spatial area objects (e.g., administrative areas, watershed, topographic areas…), constitute various characteristics at each area location (Demšar, Harris, Brunsdon, Fotheringham, & McLoone, 2012). This allows spatial comparisons between the studied areas. Furthermore, the application of this kind of statistical model became more prudent, due to the

* Lebanese University – Department of Geography – Branch 4

Digital Elevation Model (DEM). This technic, defined as a digital cartographic dataset in the three coordination (XYZ) derived from contour lines or photogrammetric method (Gandhi & Sarkar, 2016), facilitates the extraction of topographic information related to slopes.

One of the geographical studies that can be applied using the spatial PCA method is the slopes' characteristics similarity analysis. Accordingly, the eastern and western slopes of the two mountain ranges of Lebanon overlooking the Beqaa plain can be considered a typical case for such studies, due to the hypothesis that was led about their similarity by the Swiss geologist Louis Dubertret who studied the geology of the Lebanese lands. He supposes that these slopes, which face the Beqaa plain are dissimilar, especially concerning their gradient slope (Dubertret, 1932, pp. 364-365):

> *« Les pentes occidentales du Liban sont douces ; la montée se fait par flexures laissant entre elles des gradins faiblement inclinés vers l'Ouest.* ***Les retombées orientales sont abruptes ».***
> *«L'Anti-Liban a beaucoup de similitude avec le Liban.* ***Les pentes occidentales sont douces****, les retombées orientales abruptes ».*

In this context, the present paper is dedicated to answering the problem of the similarity of these slopes. Accordingly, the hypothesis that will be proven in our study is that the slopes of the western chain and their corresponding in the eastern one are not completely dissimilar.

Therefore, this study aims to divide these slopes into groups of similarity, to verify the Dubertret supposition. Moreover, the new groups that may turn out, can help the decision makers to unify any plans for any physical and human rehabilitation concerning these slopes, where exist many human activities. Furthermore, this study can facilitate the comparison of the hydrological-geomorphological process associated with erosion's evolution. Therefore, this allows us to draw up the appropriate protection plans from geomorphological risks, specifically landslides, and soil encroachments.

2. Study area

The study area includes the eastern slopes of the Mount-Lebanon chain and the western slopes of the Anti-Lebanon chain. These two ranges of slopes are separated from the western slopes and the eastern slopes of each of the two chains, by the watershed line adopted as the study area's upper limit.

On the other hand, the studied slopes are separated from each other, by the Beqaa plain extending in both the middle and the northern sides, where it appears as a wide region (about 8 Km on average). Conversely, the plain disappears starting from the Qaraaoun region along the rest of the southern side, where it transforms into a slit band that passes through the two studied slopes (figure 1). In this

context, Dubertret declares that the limit between the slopes of the two chains becomes confused and unclear in this region (Dubertret, 1932, p. 365):

« Le Liban et l'Anti-Liban n'ont pas de prolongement nettement apparent au Sud du Liban. »

Accordingly, we adopted that each area with a slope of more than 3.5 degrees was considered a part of the study area. The reason is due to that threshold represents the steepness at which a topographic turn occurs from a sloping area to a flat area. This topographic turn confirmed the topographic cross-sections of this region. All the regions between the studied slopes having a gradient below 3.5°, were considered as a part of the plain area. It was not desirable to adopt another criterion to set the lower limit, such as the altitude, for example, due to its large variety in this plain region. Consequently, this can lead to setting aside a large part of the study area. As an example, the Beqaa plain decreases from about 1100 m in Baalbek to about 840 m in the southern region of this plain, and about 600 in the northern region of it. Consequently, and let's assume that an altitude of 1000 m will be adopted as a limit, all zones below this limit on the northern and the southern sides of the studied slopes will be picked out of them.

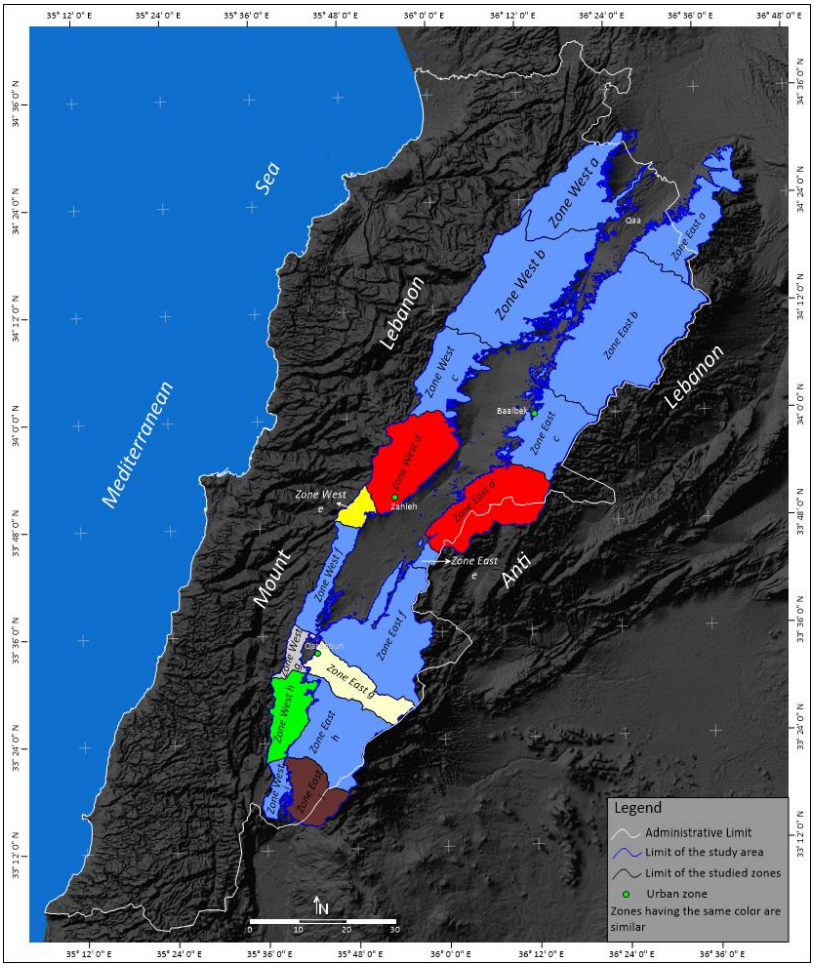

Figure1 : Map of the study area

On the other hand, the study area was divided into 18 zones of slopes: 9 of them are in the Mount-Lebanon chain, and the other 9 are in the Anti-Lebanon chain. The limit of each zone of the Mount-Lebanon chain coincides with the limit of each of its 9 mountain standard blocks. Passing by the lower elevation points, the limits separate between the following blocks, which are from northeast to southwest: the Aakkar mountain block (Zone West a), Jabal el Makmel (Zone West b), Mnaïtra (Zone West c) and Jabal Sannine (Zone West d), Jabal Knîssé (Zone West e), Jabal el Barouk (Zone West f), Jabal Niha (Zone West g), Jabal Rihâne (Zone West h), and Jabal Aamel (Zone West i). As for the limit of each zone of the 9 zones of the Anti-Lebanon chain, it was the extension of the limit of each Mont-Lebanon chain zones. These Anti-Lebanon zones were given the following names: Zone East

a, Zone East b, Zone East c, Zone East d, Zone East e, Zone East f, Zone East g, Zone East h, and Zone East i (figure 1).

As mentioned above, the 9 mountains block of Mont-Lebanon were considered as the reference for the selection of the 9 zones of Anti-Lebanon, and not the Anti-Lebanon two mountain blocks that constitute this chain (Charqi and Hermon mountains). The reason was as follows: if the blocks in this chain were used as reference instead of the Mont-Lebanon ones, we would have obtained only four zones. Accordingly, this kind of division only gives the outlines of the similarity between the studied slopes and decreases the margin of comparison between them. Contrary to the 18 zones division that gives more precise details about the similarity between these slopes.

In this study area, which formed a wide scientific debate among the researchers who studied the geology of the Lebanese lands, most notably Dubertret and De Vomas, we noticed several factors that affect the similarity of its slopes, and subsequently, make it a typical study area. One of these factors is the tectonic characteristics represented by the presence of major fault networks along these slopes. The most important are Yammoûné and Serghâyâ, which, according to Dubertret are considered an extension of the Dead Sea big fault (cf. discussion). Furthermore, a hydrologic factor can affect the similarity of these slopes; The study area constitutes the mountainous parts of 3 watersheds that feed the following rivers from the northeast to the southwest: Orontes, and Hasbani, two international rivers. In addition to Litani, the longest national river (180 Km) flows into the Mediterranean Sea. These rivers are fed by a group of tributaries that run on well-studied slopes and contribute to their erosion, such as Berdawni, Hala, El Ghzaïyel, and Qabb Elias. Additionally, we noticed the large stratigraphic diversity extending along these slopes from the Jurassic to the fourth geological time. This stratigraphic diversity was accompanied by a wide lithological diversity that allowed the presence of many types of rocks, such as lime, marl, and sandstone. Moreover, human activities form an important factor affecting the similarity of these slopes. It is represented by constructions, roads, and quarries (cf. results).

3. Materials and methods

3.1. Data

The database of this study included 12 variables of 30 others concerning the characteristics of slopes in our study area. These variables that constitute the input elements of the spatial PCA model are the only variables that satisfied the three necessary conditions to give significance to the output values of the model (cf. PCA method).

These variables are included the maximum of the tangential Curvature (TC), which measures curvature about a vertical plane perpendicular to the gradient direction, or tangential to the contour (Surfer, 2021).

In addition to the TC, the chosen variables include the minimum of the first derivative (FD). This index calculates the slope of the surface along a given direction. First derivative grid files produce contour maps that show isolines of constant slope along lines of fixed direction (Surfer, 2021).

Moreover, the minimum and the maximum of the second derivative (SD) are selected too from the 30 variables. The SD calculates the rate of change of slope along a given direction. Second derivative grid files produce contour maps that show isolines of a constant rate of change of slope across the surface (Surfer, 2021).

Furthermore, the maximum of the plan curvature (PlC). The Planform curvature (commonly called plan curvature) is perpendicular to the direction of the maximum slope. Planform curvature relates to the convergence and divergence of flow across a surface. It reflects the rate of change of the Terrain Aspect angle measured in the horizontal plane and is a measure of the curvature of contours (Evans, 1980).

One of the selected variables was the maximum gradient (Gr). It defines the steepness and the flatness of the slopes (Drăguţ & Blaschke, 2006).

This is in addition to the maximum of the profile curvature (PrC). The Profile curvature is parallel to the slope and indicates the direction of the maximum slope. It affects the acceleration and deceleration of flow across the surface. (i.e., following a streamline downstream) (Peckham, 2011).

And the maximum of the curvature (Cu), which is a positive number and can be considered as a measure of the rate of change, in a specified direction, of the inclination angle of tangential planes on a profile line (Surfer, 2021).

In addition, the selected variables include the maximum and the minimum values of the terrain ruggedness (TeR), which computes the difference between the value of each cell and the mean of an 8-cell neighborhood of surrounding cells and classifies its values in seven classes (from “level” to “extremely rugged”) (De Lamo & Shennan-Farpón, 2019).

The maximum of the roughness index (Ro) is picked from the 30 variables too as a studied variable. The Ro index reflects the irregularities in the surface texture. Surface roughness exists in two principal planes; perpendicular to the surface, described as height deviation, and in the plane of the surface, identified as texture (Whitehead & Verran, 2006).

Besides the above variables, the maximum and the minimum of the topographic index (ToI) were selected too. The ToI is defined as a measure of the extent of flow accumulation at the point of the topographic surface (Beven & Kirkby, 2009).

Because the Surfer does not include the special algorithm to calculate the last three variables we used QGIS v3.2.1 to calculate them, and always Surfer 23 to calculate the first 9 variables.

3.2. PCA method

To get an optimal result, the spatial PCA method applied in this study was based on two essential factors: the rotation method of the spatial PCA model, and the conditions that were taken into consideration to increase the accuracy of this model.

As a rotation method, we used the varimax method developed by Kaiser. This method used commonly for orthogonal rotation (Kaiser H. , 1958), maximizes the simplicity of the factor (Fiorina, Armanino, Lanteri, & Leardi, 1988) that makes it easier for interpretation. Moreover, it can be used when the factors are uncorrelated from each other. Therefore, we primarily used the Oblimin with Kaiser Normalization method to only calculate the degree of correlation between the components of the studied model. As shown in table 1, the correlation is 0.438, which is considered a low correlation and makes it possible to use the varimax method.

Table 1: Component Correlation Matrix

Component	1	2
1	1.000	.438
2	.438	1.000

Extraction Method: Principal Component Analysis.
Rotation Method: Oblimin with Kaiser Normalization.

Table 2: KMO and Bartlett's Test

Kaiser-Meyer-Olkin Measure of Sampling Adequacy.		.822
Bartlett's Test of Sphericity	Approx. Chi-Square	243.705
	df	66
	Sig.	.000

Furthermore, three conditions were taken into consideration due to their importance to determine the significance of this method. These three conditions include the determinant, the Kaiser-Meyer-Olkin Measure of Sampling Adequacy, Bartlett's Test of Sphericity, and the anti-image matrices for covariance and correlation. For the first condition, it was equal to 1.999^{E-009} i.e., above the limit of 0.00001, which indicates the absence of multicollinearity (Pearce & Yong, 2013). As for the second condition equal to 0.822, was considered adequate because it exceeded the limit of 0.600 (Almalak, et al., 2014) (table 2). As for the last condition, the test results show that the PCA is appropriate for the data due to that all values of the test are above 0.5 (Tasir, El Amin Abour, Abd Halim, & Harun, 2012).

4. Results

4.1. PCA model

4.1.1. Variance of the variables

Based on the PCA method, the variance of the studied variables is explained by the 2 first components, which their initial eigenvalues are above 1 (table 3).

The first was responsible for the explanation of 54.868%, and the second for the explanation of 27.245%, giving a cumulative total of 82.113% (Table 3).

Table 3: Total Variance Explained

Component	Initial Eigenvalues			Extraction Sums of Squared Loadings			Rotation Sums of Squared Loadings		
	Total	% of Variance	Cumulative %	Total	% of Variance	Cumulative %	Total	% of Variance	Cumulative %
1	8.619	71.828	71.828	8.619	71.828	71.828	6.584	54.868	54.868
2	1.234	10.286	82.113	1.234	10.286	82.113	3.269	27.245	82.113
3	.678	5.646	87.759						
4	.436	3.636	91.396						
5	.327	2.727	94.123						
6	.298	2.479	96.602						
7	.197	1.639	98.241						
8	.079	.662	98.903						
9	.070	.582	99.485						
10	.029	.244	99.729						
11	.024	.200	99.929						
12	.009	.071	100.000						

Thus, the loss of basic information by the model is about 18%, much less than 30%; the limit from which the model becomes insignificant (Gajjar, Kulahci, & Palazoglu, 2018; Constantin, 2014).

4.1.2. Variables correlation groups (components)

The variables' correlation groups were deduced throughout the rotated component matrix of the model (table 4). For our analysis, the limit of absolute loadings that leads to arranging the variables was set to 0.600; all loading below this limit was rejected from the analysis. This limit was selected to keep only the high correlation values. Consequently, two components were obtained: The first one is strongly correlated to the first 8 variables: maximum gradient (max_grad),

Table 4: Rotated Component Matrix

Variables	Component	
	1	2
min_secdr	-.916	
min_firstdr	-.915	
max_terugg	.882	
max_grad	.879	
max_rough	.846	
max_topin	.839	
min_topin	-.753	
max_secdr	.681	
max_plcurv		.921
max_prcurv		.733
max_curv		.711
max_teng		.605

Extraction Method: Principal Component Analysis.
Rotation Method: Varimax with Kaiser Normalization.
a. Rotation converged in 3 iterations.

maximum second derivative (max_secdr) and minimum second derivative (min_secdr), maximum topographic index (max_topin), minimum topographic index (min_topin), maximum roughness (max_rough), minimum first derivative (min_firstdr), maximum terrain ruggedness (max_terugg). Under the group named "direction slope variation variables (DSVV)", these variables are responsible for the explanation of 54.868 % of the model.

However, the second component is mostly correlated to the last 4 variables, which are: maximum plan curvature (max_plcurv), maximum profile curvature (max_prcurv), maximum curvature (max_curv), maximum tangential curvature (max_teng). These variables that can be grouped as "curvature variables (CV)" are responsible to explain 27.245 % of the model.

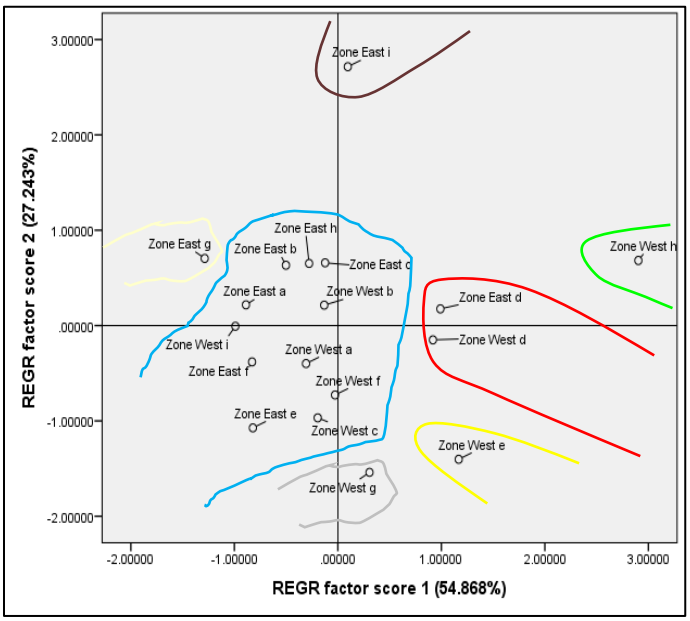

Figure 2: REGR factor scores

4.2. Cross-section similarity analysis

A general observation released through REGR factor scores (figure 2), shows the presence of 7 main groups of zones concerning the similarity of their slope's characteristics: The group surrounded by the blue line constitutes the largest group; it includes 61% of all studied slopes, such as zone West a, and East a.

Table 5: factor scores

Zones	Factor scores		Zones	Factor scores	
	1	2		1	2
Zone West a	-0.3077	-0.3991	Zone East a	-0.8877	0.21737
Zone West b	-0.1317	0.2142	Zone East b	-0.5018	0.63253
Zone West c	-0.1949	-0.9678	Zone East c	-0.1235	0.65799
Zone West d	0.91811	-0.1503	Zone East d	0.99038	0.17491
Zone West e	1.16739	-1.4027	Zone East e	-0.8216	-1.0735
Zone West f	-0.0274	-0.7284	Zone East f	-0.8292	-0.3815
Zone West g	0.30566	-1.5399	Zone East g	-1.2869	0.7036
Zone West h	2.90312	0.68285	Zone East h	-0.2777	0.65139
Zone West i	-0.9905	-0.0068	Zone East i	0.09587	2.71507

It is followed by the group surrounded by the red line, which includes only 2 zones: East d and West d. The rest 5 groups include each unique zone: the brown line includes zone East i, while the green

one includes zone West h, although the yellow one includes zone East e, and the gray line includes zone East g. Finally, the pale-yellow line includes the zone East g.

A deeper analysis of the similarity between the studied zones can be achieved based on factor scores observation. They are divided into factor score 1 referred to DSVV characteristics, and factor score 2 referred to CV characteristics (table 5).

Each of the studied zones presents a uniqueness concerning the 2-factor scores. Accordingly, the comparison between them permits us to reject the supposition of Dubertret in the northern zones, which present a remarkable similarity. Contrariwise, this analysis admits his supposition concerning most of the southern zones.

4.2.1. Northern cross-section comparison

Figure 1 notice that the northern zones' slopes (West: a, b, c, d, and East: a, b, c, d) are relatively similar to each other: except the zones, West d and East d, the values of factor 1 and factor 2 of all its western and eastern slopes reveal a remarkable similarity between them. These values, which refer to DSVV and CV are attached to the average; they don't exceed 1.

Table 6: Values of the similar studied variables

	Maximum gradient (%)	Maximum profile curvature	Maximum plan curvature	Maximum second derivative	Maximum curvature	Maximum roughness	Maximum terrain ruggedness
Zone West d	1.049649	0.595171	0.036119	0.418543	0.61884	1.1381358	0.9786292
Zone East d	1.103012	0.658655	0.003637	0.317419	0.64305	1.108359	0.9163844

Regarding zones West d and East d, which are located in the far south northern section, they appear only similar to each other, not to the rest of this section. This similarity that appears clearly in 7 studied variables (table 6) interprets their topographic outlines. So large, each zone appears as the mirror of the other zone. In the West d zone, the Berdawni River valley extends from its northeast side to its southwest one, then, deviates to the east. This valley is faced by the Hala River valley in the East d zone, which extends too from its northeast side to its southeast side, then deviates to the west (figure 3). The only difference that appears between these two valleys is represented by the depth: the Berdawni river valley is deeper than the Hala River valley by about 86 m. This difference can be explained by the fact that the permanently flowing Berdawni river, which has a maximum debit of about 13 m3/s at the beginning of June, digs a valley of about 530 meters deep in geological layers consisting of more than 90% of limestone rocks. As for the Hala River, which is an intermittent river (flows only between December and early June), and whose debit does not exceed about 2.1

m3/s, it digs a valley with an average depth of about 445 meters in a similar geological layer as the Berdawni river. The debit of each of the two rivers was revealed through a monthly field measurement during the hydrologic year 2021-2022, at the embouchure of each of them in the Litani River.

Moreover, the similarity in the topographic outlines appears in the two forefronts of the main mountain blocks of these two zones: having a length of about 21 km and a large of about 2.5 km for each one, these forefronts descend toward west and east from the watershed line of each one, with an average slope of about 10%.

Furthermore, the similarity between the slopes of these two zones is not limited to the topography but reaches out to their stratigraphy. At the contact area of each zone with the plain extend layer n2 constituted by pudding rocks. Straight up, it is followed by layer n1 formed by marl rocks, layer e2b by lime, and e2a by lime-marl. The similarity in the stratigraphy continues to the upper layers of this zones where extends the c6 layer formed by marl, then the c5 is constituted by the lime-marl stone. At the watershed line of each zone extend the c'4 layer constituted by the lime-dolomite, and the c4 a marl layer (figure 3).

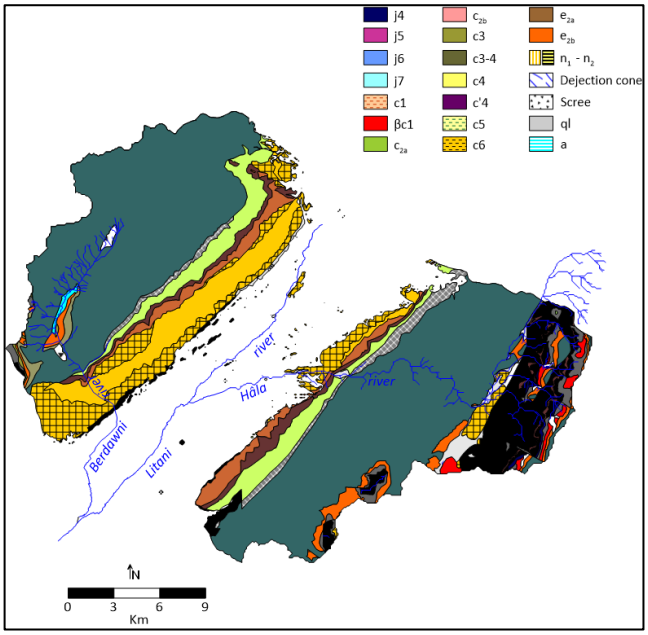

Figure 3: Similarity of the stratigraphy in zones West d and East d.

The reason for the similarity in the northern part of the studied slopes may be attributed to the limited effect of river water erosion, which reduces transportation of the rock materials, consequently, preserving the characteristics of these slopes, especially the gradient. The reason for this defined effect can be explained by the lack of rain (does not exceed 500 mm/year) that receives these slopes, due to the relatively high elevation of the Mount-Lebanon chain (about 3088 m at Kornet al-Sawda). This factor can reduce the effectiveness of the humid western air masses by preventing them from reaching these slopes. For example, the Litani River does not become a real river until it reaches the southern borders of the upper studied slopes. And that is grace to its main tributaries, namely the el Ghzaïyel River, the Berdawni River, and the Qabb Eliâs River that flow over these slopes. As for the main upper region, it is devoid of meaningful tributaries that draw its slopes.

4.2.2. Southern cross-section comparison

The similarity between the slopes of the northern cross-section zones does not cover the southern section ones, where is noticed a clear contrast between most of them; except the West f and East f zones, each of the remaining ones presents a unique characteristic in their slopes.

Starting with the uniqueness of zone West e (El Knîssé Mountain) is represented by the high values of factor 1 (1.16739), which reveal DSVV characteristics, and on the other hand by the low values of factor 2 (-1.4027), which reveal CV values.

These results may be due to human activity represented by two factors: the first one is the 10 quarries dug at the northeastern edge of zone West e, which occupies a general area of 7 Km^2. Quarries can lead to the formation of steep slopes and cliffs near the quarry (Kaiser & Kim, 2017; Malavasi, D'Ambrosio, Antonello, & Giacomini, 2018). In this zone, the chaotic extraction of the rocks due to these activities violates the rules in terms of leaving rocky terraces at the quarries' sites. Thus, the steepness of the slopes increases, and left areas with a large maximum gradient of 81%.

The second human activity is represented by the international highway dug in this area with a length of about 12 km and a width of about 300 m, which also led to decreased CV values. This road is constructed at a lower elevation than the surrounding mountain slopes, resulting in a flatter profile curvature than the natural terrain (Abdrakhmanova & Sakhautdinov, 2019; Sridevi & Ravikumar, 2015).

As for zone West g, it shows factor 1 values around the average (0.30566), as there is nothing that distinguishes it from others. While factor 2 decreases to -1.5399. The reason for the relative flatness of CV values may be due to the absence of the network of forked faults (such as zone East i) that could cause high CV values; Through the geological map of the Jezzîne region (Dubertret, 2000), we notice mainly the Yammoûné longitudinal fault that crosses this zone from the SSW to the NNE along its contact line with the plain at an altitude of about 1200 m.

Furthermore, zone East i is similar to zone west g in factor 1 values, which are centered around the mean (0.09587). Contrary, zone East i is unique with a significantly high value in factor 2 (2.71507), which is considered the highest among all the studied regions. This may be due to that this zone is crossed by two main faults, which lead to an increase in the CV values: The first fault is Hâsbaïya. It extends from the Hula region towards the northeast and stops near Hâsbaïya, passing by the feet of the Hermon Mountain range, at a height of about 600 m. Extending to the east of the first one, the second fault draws a crooked line from the Dead Sea to the NE end of the zone East g, where it is divided into two parts: the first one heads to the north, passing at the feet of Mount Hermon too with a length of 7 km. However, the second part of this fault passes through Shabaa at an altitude of about 2000 m, then head to the North where it joins Serghâyâ fault.

However, the zone West h presents a high unique value too but in factor 1 (2.90312). This highest value between all the factor 1 values of the other zones is the result of the high values of DSVV characteristics, contrary to factor 2, which has values around the average (0.68285). This case may be the result of the presence of the Litani River Valley, which excavates the deepest valley in the study area (570 m of depth) from the northeast to the southwest of this zone.

As for the role of erosion, a larger amount of rain remains, which reaches about 900 mm/year. This contributed to rich watercourses that supply the Litani and Hasbani rivers, making the erosion process relatively active. It thus creates differences in the characteristics of the slopes in this region. We mention here in particular the Chtaura River and the tributaries of the Hasbani River, which flows through Hermon Mountain.

5. Discussion

The PCA method applied in this study using the DEM database contributes to rejecting Dubertret's supposition concerning the similarity between the studied slopes. Accordingly, using such modern techniques may lead to rejecting too the entire hypothesis of Dubertret's theory about the formation of the Beqaa region extended between these two slopes. Especially that this theory was the subject of much discussion and controversy between him and other scientists, most notably De Vomas.

Lengthily, Dubertret supposes that the Beqaa region is a synclinal, which goes down between the extended faults of the Mert Morte and Jordan ditch (Dubertret, 1955; Blankenhorn & Oppenheim, 1927; Fisher, 2013; Dubertret & Weuleresse, Manuelle de Géographie: Syrie, Liban, et Proche Orient, 1940). Contrary to Dubertret, Etienne De Vaumas, a French geographer, consider that such interpretation doesn't correspond to reality; he supposes that the Beqaa region is a synclinal that extends between two continuous folds: Mount-Lebanon and Anti-Lebanon chains (André, 1949). Moreover, he considers that the faults, which are grafted along these chains constitute only secondary or even purely local accidents (De Vaumas, 1954).

On the other hand, in comparison with the occidental slopes of the Mount-Lebanon chain, we notice that the slopes of this chain in our study area are steeper in general; The occidental regions receive large amounts of precipitation, exceeding 1500 mm/year. This allows to increase in the abundance of these coastal rivers (167 m^3/s on average) that flow into the Mediterranean Sea (13 main rivers), and thus increases the effectiveness of erosion. Conversely, the slopes of the study area do not receive more than 500 mm/year as a general average, this causes a decrease in the abundance of their rivers (12 m^3/s as average) which constitute the main tributaries of the interior rivers, especially Litani River tributaries. Thusly, decreases the effectiveness of erosion.

As for the limits of this study, it is the absence of quantitative measurements of the materials carried by rivers due to the erosion process along the slopes of the studied area. These measurements are not

directly related to the subject of this study, but they contribute to proving their effects on the similarity in the southern studied slopes. In addition, the study was limited to one factor, which is the topographic factor represented by the characteristics of the slopes. It did not include other factors, such as the similarity of climate elements, fauna, and flora. This comprehensiveness helps to cover the topic from more than one side, which contributes to the generalization of its results.

Conclusion

Based on the results of this study, we can assume that the similarity extends essentially in the northeastern slopes of Mount-Lebanon and Anti-Lebanon, especially the West d and East d zones, where it is not only limited to the topographic studied variables but also extends to the stratigraphic characteristics of the area referred to. As for the dissimilarity between the southeastern and southwestern slopes, it could be due to anthropic activities, the river tributaries that feed the Litani River and increasing erosion in the southern part of the Beqaa Valley, as well as the presence of a dense fault network passing by these slopes. Accordingly, Dubertret's supposition is applicable only in the southern zones.

Moreover, in the context of the methodology used in this study, we were able to establish a criterion for separating the western and eastern mountain ranges, which is the degree of slope. This criterion is conformed with the aerial and satellite images that show the study area among the entire physical sections of Lebanon.

Furthermore, the answers in this research paper help the competent authorities to implement a human and physical rehabilitation plan for these slopes. In particular, as we have seen above, the influence of the human activities represented by the quarries, and the water network erosion that may have a fundamental role in determining the similarity between the studied slopes.

These activities could be a field for detailed future studies, especially with the possibility of an expansion of human activities with the continuous population expansion. Contrary to river erosion, that can be stopped in light of a probable hydrologic drought, resulting in any climate changes due to global warming.

References

- Abdrakhmanova, A., & Sakhautdinov, R. (2019). Issues of Design and Construction of Roads in the Mountainous Areas. *International Journal of Innovative Technology and Exploring Engineering, 8*(10), 677-680.
- Abdrakhmanova, A., & Sakhautdinov, R. (2019). Issues of Design and Construction of Roads in the Mountainous Areas. *International Journal of Innovative Technology and Exploring Engineering, 8*(10), 677-68.

- Almalak, H., Albluwi, A., Alkhelb, D., Alsaleh, H., Khan, T., Hassali, M., & Aljadhey, H. (2014). Students' attitude toward use of over the counter medicines during exams in Saudi Arabia. *Saudi Pharmaceutical Journal, 22*(2), 107-112.
- André, G. (1949). Sur la structure des Pays du Levant. *Revue de géographie jointe au Bulletin de la Société de géographie de Lyon et de la région lyonnaise, 24*(3), 279-286.
- Berry, B. (1964). Approaches to regional analysis: A synthesis. *Annals of the Association of American Geographers, 54*(1), 2-11.
- Beven, K., & Kirkby, M. (2009). A physically based, variable contributing area model of basin hydrology / Un modèle à base physique de zone d'appel variable de l'hydrologie du bassin versant. *Hydrological Sciences Journal, 24:1*, 43-69.
- Blankenhorn, M., & Oppenheim, P. (1927). *Neue beiträge zur kenntnis des Neogens in Syrien und Palästina. Geologische und Paleontologische abhandlungen, Neue Folge.* Band 15. (der ganzen reihe band 19) Heft 4.
- Constantin, C. (2014). Principal component analysis - a powerful tool in computing marketing information. *Bulletin of the Transilvania University of Braşov*, 25.
- Davis, J. (1986). *Statistics and data analysis in geology.* New York: Wiley.
- De Lamo, X., & Shennan-Farpón, Y. (2019). *ASSESSING THE RELATIVE IMPORTANCE OF FORESTS FOR WIND EROSION CONTROL QGIS V 2.18.* Cambridge: UNEP-WCMC.
- De Vaumas, E. (1954). *Le Liban: Montagne libanaise, Anti-Liban, Hermon, Haute Galilée libanaise.* Firmin-Didot.
- Demšar, U., Harris, P., Brunsdon, C., Fotheringham, A., & McLoone, S. (2012). Principal Component Analysis on Spatial Data: An Overview. *Annals of the Association of American Geographers*, 106-128.
- Drăguţ, L., & Blaschke, T. (2006). Automated classification of landform elements using object-based image analysis. *Geomorphology, 81*(3-4), 330-344.
- Dubertret, L. (1932). *La Géologie et les Mines de la France d'outre Mer.* Paris: Société d'édition: Géographiques, Maritimes et Coloniales.
- Dubertret, L. (1933). La carte géologique au millionième de la Syrie et du Liban. *Revue de Géographie physique et de Géologie dynamique*, 269-318.
- Dubertret, L. (1955). *Carte Géologique du Liban au 1/200 000e.* Beyrouth: République Libanaise ministère des travaux publics.

- Dubertret, L. (2000). *Carte géologique au 50000e. Feuille de Djezzine.* Beyrouth: Ministère des travaux publics.
- Dubertret, L. (2000). *Carte géologique au 50000e. Feuille géologique de Merdjayoun.* Beyrouth: Ministère des travaux publics.
- Dubertret, L., & Weuleresse, J. (1940). *Manuelle de Géographie: Syrie, Liban, et Proche Orient.* Imprimerie catholique.
- Evans, I. (1980). An integrated system of terrain analysis and slope mapping. *Zeitschrift für Geomorphologie, Supplementband, 36*, 274-295.
- Fiorina, M., Armanino, C., Lanteri, S., & Leardi, R. (1988). Methods of Varimax rotation in factor analysis with applications in clinical and food chemistry. *Journal of Chemometrics, 3*, 115-125.
- Fisher, W. (2013). *The Middle East: A Physical, Social and Regional Geography.* New York: Routledge Revivals.
- Gajjar, S., Kulahci, M., & Palazoglu, A. (2018). Real-time fault detection and diagnosis using sparse principal. *Journal of Process Control, 67*, 112-128.
- Gandhi, S., & Sarkar, B. (2016). *Reconnaisance and Prospecting. Essentials of Mineral Exploration and Evaluation.* Cambridge: Elsevier.
- Hägerstrand, T. (1969). Innovation diffusion as a spatial process. *Technology and Culture, 10*(3), 480-482.
- Hotelling, H. (1933). Analysis of a complex of statistical variables into principal components. *Journal of Educational Psychology, 24*(6), 417-441.
- Johnston, R. (1978). *Multivariate statistical analysis in geography.* London: Longman.
- Kaiser, H. (1958). The varimax criterion for analytic rotation in factor analysis. *Psychometricka, 23.3*, 187-200.
- Kaiser, P., & Kim, B. (2017). Slope stability analysis of a limestone quarry on the northwestern coast of Crete. *Bulletin of Engineering Geology and the Environment, 76*(1), 1-16.
- Malavasi, M., D'Ambrosio, D., Antonello, G., & Giacomini, A. (2018). Geological and geotechnical characterization of a quarry slope affected by a deep-seated gravitational slope deformation. *Bulletin of Engineering Geology and the Environment, 77*(4), 1585-1600.
- Pearce, S., & Yong, A. (2013). A beginner's Guide to Factor Analysis: Focusing on Exploratoty Factor Analysis. *Tutorials in Quantitative Methods for Psychology, 9*(2), 79-94.

- Pearson, K. (1901). On lines and planes of closest fit to systems of points in space. *Philosophical Magazine Series 6, 2*(11), 559-572.
- Peckham, S. (2011). Profile, plan and stream curvature: A simple derivation and applications. *Proceedings of Geomorphometry 4*, 27-30.
- Prasad Mishra, S., Swain, D., Laishram, M., & Taraphder, S. (2017). Multivariate Statistical Data Analysis-Principal Component Analysis (PCA). *International Journal of Livestock Research*, 60-78.
- Sridevi, K., & Ravikumar, D. (2015). Design and Analysis of Mountain Road by Using Soft Computing Techniques. *International Journal of Innovative Research in Science, Engineering, and Technology, 4*(11), 11107-11112.
- Surfer, T. (2021). *Surfer user's guide: Powerful contouring, gridding & surface mapping system.* Colorado: Golden Software, LLC.
- Tasir, Z., El Amin Abour, K., Abd Halim, N., & Harun, J. (2012). Relationship between Teachers' ICT Competency, Confidence Level, and Satisfaction toward ICT Training Programmes: A Case Study among Postgraduate Students. *Turkish Online Journal of Educational Technology, 11*(1), 138-144.
- Tinkler, K. (1972). The physical interpretation of eigenfuctions of dichotomous matrices. *Transactions of the Institute of British Geographers, 55*, 17-46.
- Whitehead, K., & Verran, J. (2006). The Effect of Surface Topography on the Retention of Microorganisms. *Food and Bioproducts Processing*, 253-259.